### Title
An Analysis of Two-User Uplink Asynchronous Non-orthogonal Multiple Access Systems.




### Authors
Zou, Xun
He, Biao
Jafarkhani, Hamid



### Publication Date
2019

### DOI
10.1109/TWC.2019.2892486

Peer reviewed

# An Analysis of Two-User Uplink Asynchronous Non-Orthogonal Multiple Access Systems

Xun Zou, *Student Member, IEEE*, Biao He, *Member, IEEE*, and Hamid Jafarkhani, *Fellow, IEEE*

**Abstract**

Recent studies have numerically demonstrated the possible advantages of the asynchronous non-orthogonal multiple access (ANOMA) over the conventional synchronous non-orthogonal multiple access (NOMA). The ANOMA makes use of the oversampling technique by intentionally introducing a timing mismatch between symbols of different users. Focusing on a two-user uplink system, for the first time, we analytically prove that the ANOMA with a sufficiently large frame length can always outperform the NOMA in terms of the sum throughput. To this end, we derive the expression for the sum throughput of the ANOMA as a function of signal-to-noise ratio (SNR), frame length, and normalized timing mismatch. Based on the derived expression, we find that users should transmit at full powers to maximize the sum throughput. In addition, we obtain the optimal timing mismatch as the frame length goes to infinity. Moreover, we comprehensively study the impact of timing error on the ANOMA throughput performance. Two types of timing error, i.e., the synchronization timing error and the coordination timing error, are considered. We derive the throughput loss incurred by both types of timing error and find that the synchronization timing error has a greater impact on the throughput performance compared with the coordination timing error.

**Index Terms**

Non-orthogonal multiple access, asynchronous transmission, oversampling, timing mismatch, interference cancellation.

Results in this paper were presented in part at the IEEE International Conference on Communications (ICC) 2018 [1]. This work was supported in part by the NSF Award CCF-1526780.

The authors are with the Center for Pervasive Communications and Computing, Department of Electrical Engineering and Computer Science, University of California, Irvine, CA, 92697 USA (email: {xzou4, biao.he, hamidj}@uci.edu).

# I. INTRODUCTION

Non-orthogonal multiple access (NOMA) is envisaged as a promising technique for future radio access [2]. Traditional orthogonal multiple access (OMA) techniques allocate orthogonal resources to different users, e.g., orthogonal time resources in the time division multiple access (TDMA) scheme. Differently, the NOMA provides the multiuser access by allocating non-orthogonal resources to users [3]. For example, in the power-domain NOMA scheme, the signals for multiple users are superposed at different power levels using superposition coding [4], and the multiuser detection method, such as successive interference cancellation (SIC) [5], is employed at the receiver. The advantages of the NOMA over the OMA have been extensively studied in [2] and the references therein, e.g., providing higher system throughput compared with OMA and supporting massive connectivity.

Another line of research is to study the effects of asynchronous transmission on the performance of the wireless communication systems. Asynchronous transmission refers to the case where the symbol epochs of the signals transmitted by the users are not aligned at the receiver [6]. In particular, [6] first pointed out the potential advantages of symbol-asynchronous communications in terms of increasing the capacity of a multiple-access channel. The work in [7] applied the symbol-asynchronous channel estimation method to tackle the pilot contamination problem in massive multiple-input multiple-output (MIMO) systems. Asynchronous transmission was studied in [8, 9] as a tool to mitigate or cancel the inter-user interference. In addition, the nonzero symbol offset was used to reduce the inter-antenna interference in MIMO systems in [10]. Moreover, an asynchronous analog network coding scheme for multiuser cooperative communications was proposed in [11] to provide a greater diversity order compared with that of synchronous analog network coding. Also, adding intentional timing mismatch was proposed in [12] to improve the performance of a relay network. The authors of [13, 14] further proposed several differential decoding schemes for asynchronous multiuser MIMO systems based on orthogonal space-time block codes (OSTBCs) and for differential distributed space-time coding systems with imperfect synchronization.

The asynchronous transmission has also been studied in physical-layer network coding (PLNC). In PLNC, the two end nodes send signals simultaneously to the relay in the first time slot, where the symbol misalignment is inevitable. A general framework for decoding at the receiver based on belief propagation was investigated in [15], which can effectively deal with symbol

and phase asynchronies while incorporating channel coding at the same time. The implementable techniques used in PLNC were manifested in [16], which estimate time and frequency offsets, and detect information symbols at the relay. In [17], an optimal symbol-misalignment estimator for asynchronous PLNC was designed and the impact of misalignment-estimation error on a channel-coded PLNC system was studied. First, we highlight that the existing work in asynchronous PLNC and our work in this paper apply to different scenarios with different system setups. Second, most of the existing work in asynchronous PLNC adopts the bit/symbol/frame error rate as the performance metric. The throughput performance studied in this paper has not been addressed. Third, the key idea of the existing work in asynchronous PLNC is to estimate and then reduce the negative effect of or take advantage of the symbol misalignment while the timing mismatch is considered to be intentionally added in this paper. Thus, the optimal system design, including the optimal transmit power and timing mismatch, and the impact of timing error on NOMA have not been studied prior to this work.

Applying the symbol-asynchronous transmission to NOMA, a scheme named asynchronous NOMA (ANOMA) was studied in [18]. In fact, an idea similar to the ANOMA in [18], i.e., applying asynchronous transmission for multiple access, has also been proposed and investigated in, e.g., [8, 9, 12]. Specially, a timing mismatch between signals for different users is intentionally added as an additional resource to address the problem of inter-user interference. It has been shown using the numerical simulation in [18] that the ANOMA outperforms the conventional (synchronized) NOMA by achieving a larger throughput.

However, the work in [18] has several limitations. While addressing those limitations is important to understand the ANOMA systems, to the best of our knowledge, no existing paper has tackled the following issues. First, there is no analytical result on the comparison between the performance of the ANOMA and that of the NOMA in terms of the throughput, although numerically it is shown that ANOMA outperforms NOMA in certain scenarios. This is probably because the existing expression for the throughput of the ANOMA system is given as a function of the channel matrix but not the signal-to-noise ratio (SNR). The lack of such an expression in terms of SNR makes the analytical comparison between NOMA and ANOMA almost intractable. Second, the optimal design of ANOMA has not been investigated. Despite the fact that the performance of ANOMA is directly affected by important design parameters such as the transmit power and the timing mismatch, existing papers mainly focused on the performance demonstration only. Third, the impact of timing error has not been studied on the ANOMA

systems. In the ANOMA systems, existing studies ideally assumed that the timing information was perfectly known. However, the timing information in practice cannot always be perfectly obtained, and the timing error is often inevitable. The timing information plays a vital role in ANOMA systems, since oversampling is designed using the timing information [7, 8]. Note that the impact of timing error has been widely studied on different communication systems, such as [19] on the direct-sequence code division multiple-access (DS-CDMA) system, [20] on the multi-carrier code division multiple-access (MC-CDMA) system, and [21] on the multiple-input single-output (MISO) system using distributed OSTBC to name a few.

In this paper, we comprehensively investigate the ANOMA in a two-user uplink system. The primary contributions of the paper are summarized as follows:

1) For the first time, we analytically prove that the ANOMA with a sufficiently large frame length can always outperform the NOMA in terms of the system sum throughput. To this end, we derive the expression for the sum throughput of the ANOMA system as a function of SNR, frame length, and normalized timing mismatch. A simplified throughput expression is further obtained for the asymptotic case of infinite frame length.
2) We investigate the optimal design of the two-user uplink ANOMA system aiming at maximizing the sum throughput. We find that each user should transmit at full power despite the negative effect of inter-user interference. In addition, we prove that the optimal timing mismatch converges to one half of a symbol time as the frame length goes to infinity.
3) We analyze the impact of timing error on the performance of the uplink ANOMA system. Two types of timing error are taken into consideration, i.e., the synchronization timing error and the coordination timing error, which account for the timing error caused in signal synchronization and the coordination of the timing mismatch between asynchronous signals, respectively. We derive the expressions for the throughput loss of the ANOMA system with respect to both types of timing error, and analyze how the synchronization timing error and the coordination timing error individually and jointly affect the system performance.

Compared with our conference version [1] which briefly analyzed the impact of timing error in the ANOMA systems, the new analyses incorporated in this paper include, e.g., the sum throughput analysis of the ANOMA, the analytical comparisons between ANOMA and NOMA,

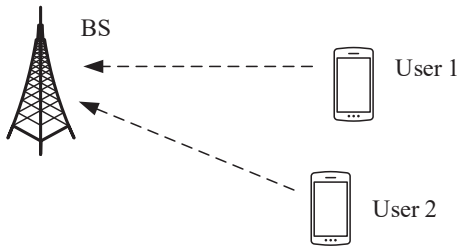


Fig. 1: Illustration of a two-user uplink system.

the asymptotic analysis for a large frame length, and the optimal transmit power and timing mismatch designs. The remainder of the paper is organized as follows. The two-user uplink system model is presented in Section II. The performance of the ANOMA system is analyzed in Section III. We discuss the optimal design of the ANOMA system in Section IV. We analyze the outputs of ANOMA matched filters with timing error and the throughput loss incurred by timing error in Section V. Numerical results are presented in Section VI. Finally, we draw the conclusions in Section VII.

Notations: $(\cdot)^H$ denotes the Hermitian transpose, $(\cdot)^T$ denotes the transpose, $\mathrm{Tr}(\cdot)$ denotes the trace operation, $(\cdot)^{-1}$ denotes the inverse operation, $|x|$ denotes the absolute value of $x$, $\mathbb{E}[\cdot]$ denotes the expectation operation, $\mathcal{CN}(0,1)$ denotes the complex normal distribution with zero mean and unit variance, and $\mathbf{1}(\cdot)$ denotes the unit step function whose value is zero for negative arguments and one for positive arguments.

## II. System Model

In this paper, we consider an uplink system which consists of a single base station (BS) and two users, as shown in Fig. 1. The two users share the same frequency-time resource to transmit signals to the BS. We assume that perfect channel state information (CSI) is known at the BS via the uplink channel training.

### *A. ANOMA System*

For the ANOMA, a timing mismatch is intentionally introduced between the symbols from two users. By intentionally introducing the timing mismatch, the oversampling technique can be adopted at the receiver, so that extra linearly independent samples can be obtained to have sampling diversity. Then, the performance of the ANOMA can be improved by utilizing the

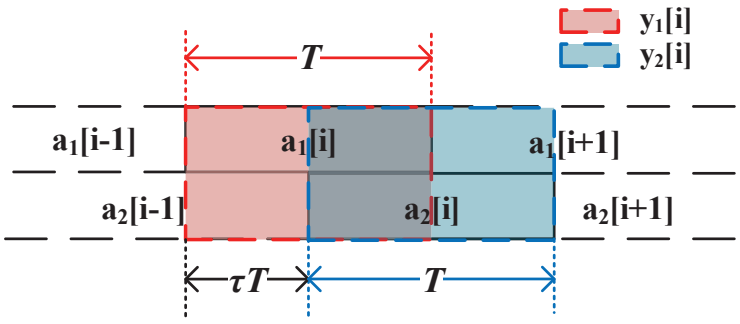


Fig. 2: Illustration of the sampling for ANOMA.

sampling diversity. In contrast, one cannot get sampling diversity by oversampling the synchronized signals in conventional NOMA schemes. As shown in Fig. 2, the intended timing mismatch between the symbols of Users 1 and 2 is denoted by $\tau T$, where $T$ is the duration of each symbol and $\tau$, $0 \leq \tau < 1$, is the normalized timing mismatch. Note that the ANOMA system becomes a synchronous NOMA system when $\tau = 0$. In this section, we assume that $\tau$ is perfectly known at BS via timing offset estimation and uplink timing control techniques, such as the timing advance [22]. We will study the ANOMA system with timing error in Section V.

Let $a_1[i] = h_1\sqrt{P_1}s_1[i]$ and $a_2[i] = h_2\sqrt{P_2}s_2[i]$, where the subscripts 1 and 2 denote the parameters for Users 1 and 2, respectively, $s_j[i]$ $(j = 1, 2)$ denotes the $i$th normalized transmitted symbol, $h_j$ denotes the channel coefficient in the block of transmission, and $P_j$ denotes the transmit power. The BS's received signal at time $t$ is then given by

$$y(t) = \sum_{i=0}^{N-1} a_1[i]p(t - iT) + \sum_{i=0}^{N-1} a_2[i]p(t - iT - \tau T) + n(t), \tag{1}$$

where $N$ denotes the number of symbols in a frame, i.e., the frame length, $T$ denotes the time duration of one symbol, $p(\cdot)$ denotes the pulse-shaping filter, and $n(t) \sim \mathcal{CN}(0, 1)$ denotes the normalized additive white Gaussian noise (AWGN). Without loss of generality, the rectangular pulse shape is adopted, i.e., $p(t) = 1/\sqrt{T}$ when $t \in [0, T]$ and $p(t) = 0$ when $t \notin [0, T]$. With the block fading model, we assume that the channels remain static during the transmission of $N$ consecutive symbols. As an initial study on the ANOMA systems, our paper adopts a basic flat fading channel model without the consideration of a frequency selective channel and OFDM. The assumption of flat fading has been widely used in the existing literature; see, e.g., [3, 10, 16, 18], and the references therein.

The BS uses the oversampling technique to take advantage of sampling diversity in the asynchronous systems [1, 7]. Oversampling uses the matched filter to sample signals at instants $iT$ and $(i+\tau)T$, $i = 1, \cdots, N$, which produces $2N$ samples without doubling the sampling rate. It has been shown in [6] that the samples obtained by oversampling are sufficient statistics for the transmitted messages in the symbol-asynchronous scenario.

As shown in Fig. 2, the BS obtains two sample vectors, denoted by $[y_1[1], \cdots, y_1[N]]^T$ and $[y_2[1], \cdots, y_2[N]]^T$. Specifically, the $i$th element in the first sample vector is given by

$$\begin{aligned} y_1[i] &= \int_0^\infty y(t)p(t-iT)dt \\ &= \int_0^\infty a_1[i]p(t-iT)p(t-iT)dt \\ &+ \int_0^\infty \{a_2[i-1]p(t-(i+1+\tau)T) + a_2[i]p(t-(i+\tau)T)\}\, p(t-iT)dt + n_1[i] \\ &= a_1[i] + \tau a_2[i-1] + (1-\tau)a_2[i] + n_1[i], \end{aligned} \tag{2}$$

where $n_1[i] = \int_0^\infty n(t)p(t-iT)dt$ denotes the additive noise in the first sampled vector. The $i$th element in the second sample vector is given by

$$y_2[i] = \int_0^\infty y(t)p(t-iT-\tau T)dt = a_2[i] + \tau a_1[i+1] + (1-\tau)a_1[i] + n_2[i], \tag{3}$$

where $n_2[i] = \int_0^\infty n(t)p(t-iT-\tau T)dt$ denotes the additive noise in the second sampled vector. From (2) and (3), we note that the inter-user interference exists, since the symbols for Users 1 and 2, i.e., $a_1[i]$ and $a_2[i]$, are added together to interfere with each other in the received samples.

We can write the outputs at the BS in a matrix form as

$$\mathbf{Y} = \mathbf{RHX} + \mathbf{N}, \tag{4}$$

where

$$\mathbf{Y} = [y_1[1]\ y_2[1]\ y_1[2]\ y_2[2]\ \cdots\ y_1[N]\ y_2[N]]^T, \tag{5}$$

$$\mathbf{X} = [s_1[1]\ s_2[1]\ s_1[2]\ s_2[2]\ \cdots\ s_1[N]\ s_2[N]]^T, \tag{6}$$

$$\mathbf{N} = [n_1[1]\ n_2[1]\ n_1[2]\ n_2[2]\ \cdots\ n_1[N]\ n_2[N]]^T, \tag{7}$$

$$\mathbf{R} = \begin{bmatrix} 1 & 1-\tau & 0 & \cdots & \cdots & 0 \\ 1-\tau & 1 & \tau & 0 & \cdots & 0 \\ 0 & \tau & 1 & 1-\tau & \cdots & 0 \\ \vdots & \ddots & \ddots & \ddots & \ddots & \vdots \\ 0 & \cdots & 0 & \tau & 1 & 1-\tau \\ 0 & \cdots & \cdots & 0 & 1-\tau & 1 \end{bmatrix}, \tag{8}$$

and

$$\mathbf{H} = \begin{bmatrix} h_1\sqrt{P_1} & & & & \\ & h_2\sqrt{P_2} & & & \\ & & \ddots & & \\ & & & h_1\sqrt{P_1} & \\ & & & & h_2\sqrt{P_2} \end{bmatrix}. \tag{9}$$

We note that the inter-user interference is represented in matrix $\mathbf{R}$. If there is no inter-user interference, $\mathbf{R}$ becomes a diagonal matrix. With inter-user interference, $\mathbf{R}$ is given as (8) which is a tridiagonal matrix, but not a diagonal matrix.

We assume that the transmitted symbols are independent, such that $\mathbb{E}\left[\mathbf{X}\mathbf{X}^H\right] = \mathbf{I}$. Note that the noise terms in (4) are colored due to the oversampling, and we have

$$\mathbb{E}\left\{n_1[i]n_2^H[i]\right\} = \int_0^\infty \int_0^\infty \mathbb{E}\left\{n(t)n^H(s)\right\} p\left(t - iT\right) p\left(s - iT - \tau T\right) dtds = 1 - \tau. \tag{10}$$

Thus, the covariance matrix of $\mathbf{N}$ is given by

$$\mathbf{R}_\mathbf{N} = \mathbb{E}\left\{\mathbf{N}\mathbf{N}^H\right\} = \mathbf{R}. \tag{11}$$

As an initial study on ANOMA, the analysis in this paper focuses on the rectangular pulse shape. It is worth mentioning that the ANOMA with oversampling is also applicable to other pulse shapes, such as the raised cosine pulse shape. Since the raised cosine pulse shape spans more than $T$, it causes more severe inter-user interference compared with the rectangular pulse shape. In terms of the mathematical expression, the matrix $\mathbf{R}$ in (8) changes accordingly while (11) still holds. The $(i, j)$th entry of $\mathbf{R}$ for the raised cosine pulse shape is given as

$$\mathbf{R}_{i,j} = \begin{cases} \rho\left(\tau T + \lfloor\frac{j-i}{2}\rfloor T\right), & i \text{ is odd, } j \text{ is even} \\ \rho\left(\tau T + \lfloor\frac{i-j}{2}\rfloor T\right), & i \text{ is even, } j \text{ is odd} \\ \rho\left(\frac{j-i}{2}T\right), & \text{otherwise,} \end{cases} \tag{12}$$

where $\rho$ is the auto-correlation function of the raised cosine function. The rest of the throughput formulas remain the same.

### *B. Benchmark System – NOMA*

By setting $\tau = 0$, the ANOMA system becomes the synchronous NOMA system. For the NOMA, the BS uses the typical matched filter instead of the oversampling technique, and the $i$th sample at the BS can be written as

$$y[i] = a_1[i] + a_2[i] + n[i], \tag{13}$$

where $n[i] = \int_0^\infty n(t)p(t-iT)dt$. Note that (13) can be derived from either (2) or (3) by letting $\tau = 0$.

It is worth mentioning that the OMA systems also have the asynchrony issue in practice. For OMA, different users transmit signals using orthogonal resources. For TDMA, orthogonal time resources are allocated to different users. The asynchrony in time domain will destroy such orthogonality, which will then degrade the system performance. For orthogonal frequency division multiple access (OFDMA), orthogonal frequency resources are allocated to different users. The asynchrony in frequency domain, for example in the form of frequency offsets, will destroy such orthogonality, which will then degrade the system performance. In general, the asynchrony does not benefit the OMA schemes.

## III. Performance Analysis of ANOMA Systems

In this paper, we employ the widely used performance metric, i.e., the sum throughput, to investigate the rate performance limit of the ANOMA systems. From (4), the sum throughput of the two-user uplink ANOMA system can be written as

$$R^{\mathrm{ANOMA}} = \frac{1}{N+\tau} \log\det\left(\mathbf{I}_{2N} + \mathbf{H}\mathbf{H}^H\mathbf{R}\right). \tag{14}$$

Some existing papers, e.g., [18], define the throughput of ANOMA as

$$R^{\mathrm{ANOMA}}_{\mathrm{exist}} = \frac{1}{N} \log\det\left(\mathbf{I}_{2N} + \mathbf{H}\mathbf{H}^H\mathbf{R}\right), \tag{15}$$

which is slightly different from (14). Although (14) and (15) converge to the same expression as $N \to \infty$, we highlight that our adopted expression in (14) is more accurate than (15) for evaluating the throughput of ANOMA with finite frame length $N$, since the system actually spends $N+\tau$ instead of $N$ symbol times to transmit $N$ symbols for each user.

It is worth mentioning that the practical transmission scheme may even simply allocate $N+1$ instead of $N+\tau$ symbol times for the transmission, and the throughput becomes $R^{\mathrm{ANOMA}}_{N+1} = \frac{1}{N+1} \log\det\left(\mathbf{I}_{2N} + \mathbf{H}\mathbf{H}^H\mathbf{R}\right)$. Our analysis is still applicable to that case, since one can simply revise (most) results according to $R^{\mathrm{ANOMA}}_{N+1} = \frac{N+\tau}{N+1} R^{\mathrm{ANOMA}}$. It is also worth mentioning that (14) and (15) are based on two main assumptions. The first assumption is the symbol-level asynchrony. That is, there is a timing mismatch $\tau T$ ($\tau \in [0,1)$) between symbols from different users. The second assumption is that the timing mismatch is perfectly known at BS, which is a common assumption in the existing literature, e.g., [8, 10, 18]. We will analyze the impact of timing error in the case that the timing information is not perfectly known in Section V.

In the following theorem, we derive the sum throughput of the two-user uplink ANOMA system in terms of the receive SNRs, $\mu_1 = P_1|h_1|^2$ and $\mu_2 = P_2|h_2|^2$, the normalized timing mismatch, $\tau$, and the frame length, $N$.

*Theorem 1:* The sum throughput of the two-user uplink ANOMA system is derived as

$$R^{\mathrm{ANOMA}} = \frac{N}{N+\tau}\log\left(\mu_1\mu_2\right) + \frac{1}{N+\tau}\log\frac{(r_1^{N+1} - r_2^{N+1}) + \tau^2(r_1^N - r_2^N)}{r_1 - r_2}, \tag{16}$$

where

$$r_1 = \frac{\mu_1^{-1}+\mu_2^{-1}+\mu_1^{-1}\mu_2^{-1}+2\tau(1-\tau)+\sqrt{\left[\mu_1^{-1}+\mu_2^{-1}+\mu_1^{-1}\mu_2^{-1}+2\tau(1-\tau)\right]^2-4\tau^2(1-\tau)^2}}{2}, \tag{17}$$

$$r_2 = \frac{\mu_1^{-1}+\mu_2^{-1}+\mu_1^{-1}\mu_2^{-1}+2\tau(1-\tau)-\sqrt{\left[\mu_1^{-1}+\mu_2^{-1}+\mu_1^{-1}\mu_2^{-1}+2\tau(1-\tau)\right]^2-4\tau^2(1-\tau)^2}}{2}. \tag{18}$$

*Proof:* See Appendix A. ■

Based on Theorem 1, we present the throughput of the two-user uplink ANOMA system for the asymptotic case of $N \to \infty$ in the following corollary, which characterizes the limiting performance of the system when the frame length $N$ is large.

*Corollary 1:* The throughput of the two-user uplink ANOMA system in the asymptotic case of $N \to \infty$ is given by

$$\lim_{N\to\infty} R^{\mathrm{ANOMA}} = \log\left(\mu_1\mu_2 r_1\right). \tag{19}$$

*Proof:* See Appendix B. ■

### *A. Comparison with NOMA*

In NOMA systems, SIC is adopted at BS to decode transmitted symbols, which works as follows. The BS first decodes the message from User 1 (stronger user) while treating the codeword from User 2 (weaker user) as an extra source of interference or noise. Then, the BS subtracts the decoded message from the received signal, and decodes the message from User 2.

According to (13), with perfect SIC at BS, the sum throughput of the two users in the uplink NOMA system can be written as [23]

$$R^{\mathrm{NOMA}} = \log(1 + P_1|h_1|^2 + P_2|h_2|^2) = \log(1 + \mu_1 + \mu_2), \tag{20}$$

which can also be obtained from (16) by setting $\tau = 0$.

Due to the complicated expression for the throughput of ANOMA in (16), it is difficult to analytically compare the NOMA with the ANOMA for a general value of $N$. Instead, we provide numerical results in Section VI and consider the asymptotic case of $N \to \infty$ for an analytical comparison in the following theorem. Our asymptotic analysis here aims to provide useful insights for ANOMA in the scenario where the frame length, $N$, is relatively large. Most results in the paper are valid for any arbitrary value of $N$, e.g., the throughput analysis, the optimal transmit power design, and the impact of timing error.

*Theorem 2:* The two-user uplink ANOMA system as $N \to \infty$ achieves an equal or higher throughput compared with the NOMA system, i.e.,

$$\lim_{N\to\infty} R^{\mathrm{ANOMA}} \geq R^{\mathrm{NOMA}}, \tag{21}$$

where $\lim_{N\to\infty} R^{\mathrm{ANOMA}} = R^{\mathrm{NOMA}}$ if and only if the normalized timing mismatch $\tau = 0$.

*Proof:* See Appendix C. ■

We note that the oversampling in ANOMA enables the sampling diversity, which leads to the possible performance advantage of the ANOMA compared with the NOMA. On the other hand, an extra $\tau T$ time resource is used to transmit $N$ symbols in the ANOMA, which has a negative effect on the performance of the ANOMA compared with that of the NOMA. When $N$ is small, the negative effect of the extra transmission time dominates the sum throughput of ANOMA. As $N$ grows, the effect of the extra transmission time becomes negligible and the sampling diversity dominants, which results in Theorem 2. Thus, one can expect a better ANOMA throughput performance compared with the NOMA when $N$ is larger than a certain value.

The physical meaning of (21) is further clarified by the following corollary.

*Corollary 2:* With a sufficiently large frame length, the ANOMA outperforms the NOMA for the two-user uplink system in terms of the sum throughput.

In general, the ANOMA system requires a higher detection complexity compared with the NOMA system. ANOMA adopts the oversampling technique to obtain more samples of the signal compared with the conventional NOMA system. Thus, the decoding process of the ANOMA system involves a larger number of samples compared with that of the NOMA system. Maximum-likelihood sequence detection, with relatively high complexity, can be used to decode the transmitted messages. For the low-complexity decoding methods in the ANOMA systems,

one can employ the methods in the existing literature with some modifications, e.g., SIC with hard decision passing and the forward backward belief propagation detection proposed in [8] or the low complexity decoder using dynamic programming in [13].

## IV. Design of ANOMA Systems

From the analysis in Section III, we note that the throughput performance of the uplink ANOMA system is directly determined by the transmit powers and the normalized timing mismatch, i.e., $P_1, P_2$, and $\tau$. In this section, we investigate the optimal $P_1, P_2$, and $\tau$ that maximize the throughput of the system.

The design problem is formulated as follows:

$$\underset{P_1,P_2,\tau}{\arg\max} \;\; R^{\mathrm{ANOMA}}, \quad s.t. \;\; 0 \leq \tau < 1, \; 0 \leq P_1 \leq P_{1,\max}, \; 0 \leq P_2 \leq P_{2,\max}, \tag{22}$$

where $P_{1,\max}$ and $P_{2,\max}$ are the maximum available powers at which Users 1 and 2 can transmit, respectively. Note that the transmit powers are coupled together in a complicated way in the expression for the throughput of the ANOMA system in (16), which is different from the case of NOMA in (20). Thus, the optimal transmit powers for the ANOMA system are not easy to determine, while it is easy to find that we shall use the maximum available transmit powers at users for the NOMA system.

It is worth mentioning that the performance of the uplink ANOMA system is also affected by the frame length, $N$. However, the frame length is constrained by the channel condition, i.e., the length of each block of the block fading channel, and the acceptable transceiver complexity. Hence, we do not investigate the design of $N$ in this work and assume that it is fixed based on the channel conditions and the overall system design.

### A. Optimal Transmit Power

We first obtain the optimal transmit power scheme. We summarize the optimal transmit powers for the ANOMA system as follows.

*Theorem 3:* For the two-user uplink ANOMA system with any frame length, $N$, and the normalized timing mismatch, $\tau$, the optimal transmit powers at Users 1 and 2, $P_1^*$ and $P_2^*$, are equal to the maximum available powers at which Users 1 and 2 can transmit, $P_{1,\max}$ and $P_{2,\max}$, i.e., $P_1^* = P_{1,\max}$ and $P_2^* = P_{2,\max}$

*Proof:* See Appendix D. ■

From Theorem 3, we find that the optimal design of transmit powers for the two-user uplink ANOMA system is the same as that for the NOMA system.

### B. Optimal Normalized Timing Mismatch

We now study the optimal normalized timing mismatch, $\tau^*$. The optimal normalized timing mismatch, $\tau^*$, is analytically intractable for a general finite frame length $N$, while we can numerically obtain $\tau^*$ for a given finite $N$ by simply searching in the range of $0 \leq \tau < 1$. In addition, we present $\tau^*$ in the asymptotic case of $N \to \infty$ in the following theorem.

*Theorem 4:* For the two-user uplink ANOMA system with the frame length $N \to \infty$, the optimal normalized timing mismatch to maximize the sum throughput is given by $\tau^* = 0.5$.

*Proof:* See Appendix E. ■

## V. Impact of Timing Error on ANOMA systems

The analysis in the previous sections is based on the assumption that the BS perfectly knows the timing information. However, the timing information cannot always be perfectly obtained in practice, and the timing error is often inevitable. In this section, we study the impact of timing error on the ANOMA system.

### A. Timing Error

We consider two types of timing error for the ANOMA system, i.e., the synchronization timing error and the coordination timing error.

*1) Synchronization Timing Error:* To synchronize the signals, we need a reference signal. Without loss of generality, we use the signal from User 1 as the timing reference (the timing offset is 0). This requires a symbol-level timing synchronization with User 1 at the BS, as it is also done in NOMA. The normalized synchronization timing error, denoted by $\epsilon_1$ in Fig. 3, is due to the imperfect timing synchronization. Without loss of generality, we assume that $\epsilon_1 \in (\tau - 1, \tau)$. With the synchronization timing error, $y_1[i]$ is taken from the time $(i-1)T + \epsilon_1 T$ to $iT + \epsilon_1 T$ and $y_2[i]$ is taken from the time $(i-1)T + (\tau + \epsilon_1)T$ to $iT + (\tau + \epsilon_1)T$, although the BS intends to take $y_1[i]$ from the time $(i-1)T$ to $iT$ and $y_2[i]$ from the time $(i-1)T + \tau T$ to $iT + \tau T$. We will study the effect of this timing error later.

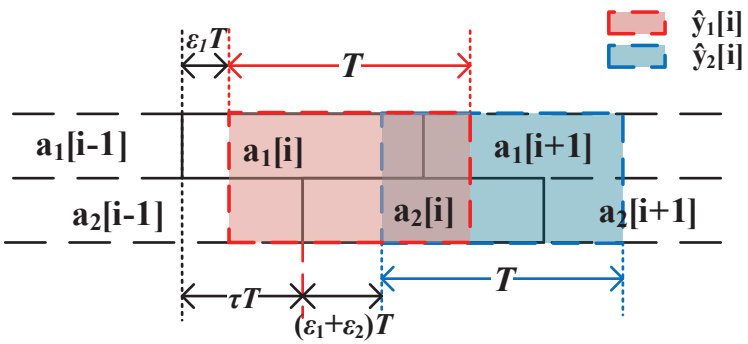


Fig. 3: Illustration of the sampling for ANOMA with timing error.

*2) Coordination Timing Error:* In order to achieve the desired timing mismatch between the two signals, the BS coordinates the uplink transmission timing of the two users to add the intended timing offsets at each transmitter. For example, the timing advance is the technique employed in long term evolution (LTE) systems to estimate and adjust the timing offsets among uplink signals at BS [22, 24]. The normalized coordination timing error, denoted by $\epsilon_2$ in Fig. 3, results from the imperfect coordination between the users. With the coordination timing error, the actual timing mismatch becomes $(\tau+\epsilon_2)T$, while the intended timing mismatch is $\tau T$. In addition to the synchronization timing error $\epsilon_1 T$, the sample $y_2[i]$ is taken from $(i-1)T+(\tau+\epsilon_1+\epsilon_2)T$ to $iT+(\tau+\epsilon_1+\epsilon_2)T$, although the BS intends to take $y_2[i]$ from $(i-1)T+\tau T$ to $iT+\tau T$. Without loss of generality, we assume that $\epsilon_1+\epsilon_2 \in (-\tau, 1-\tau)$.

Fig. 3 illustrates the sampling for an ANOMA system with timing error. It is worth mentioning that the sign of the timing error stands for the direction in which the function of the matched filter is shifted. For example, as shown in Fig. 3, the matched filter is shifted to the right by $\epsilon_1 T$ if $\epsilon_1 > 0$ compared with the matched filter designed with no timing error in Fig. 2. Fig. 3 only presents the case when $\epsilon_1 > 0$ and $\epsilon_1+\epsilon_2 > 0$, while our analysis works for any values of $\epsilon_1$ and $\epsilon_2$.

### *B. Outputs of ANOMA Matched Filters with Timing Error*

In the presence of timing error, the $i$th element of the first sample vector is given by

$$\begin{aligned}\hat{y}_1[i] &= \int_0^\infty y(t)p(t-iT-\epsilon_1 T)dt \\ &= \int_0^\infty a_1[i]p(t-iT)p(t-iT-\epsilon_1 T)dt\end{aligned}$$

$$
\begin{aligned}
&+ \mathbf{1}(-\epsilon_1) \int_0^\infty a_1[i-1]p(t-(i-1)T)p(t-iT-\epsilon_1 T)dt \\
&+ \mathbf{1}(\epsilon_1) \int_0^\infty a_1[i+1]p(t-(i+1)T)p(t-iT-\epsilon_1 T)dt \\
&+ \int_0^\infty a_2[i-1]p(t-\tau T-(i-1)T)p(t-iT-\epsilon_1 T)dt \\
&+ \int_0^\infty a_2[i]p(t-\tau T-iT)p(t-iT-\epsilon_1 T)dt + \int_0^\infty n(t)p(t-iT-\epsilon_1 T)dt \\
&= a_1[i](1-|\epsilon_1|) + a_1[i-1]\mathbf{1}(-\epsilon_1)(-\epsilon_1) + a_1[i+1]\mathbf{1}(\epsilon_1)\epsilon_1 \\
&+ a_2[i-1](\tau-\epsilon_1) + a_2[i](1-\tau+\epsilon_1) + \hat{n}_1[i], \qquad (23)
\end{aligned}
$$

and the $i$th element of the second sample vector is given by

$$
\begin{aligned}
\hat{y}_2[i] &= \int_0^\infty y(t)p(t-(i+\tau+\epsilon_1+\epsilon_2)T)dt \\
&= a_2[i](1-|\epsilon_1+\epsilon_2|) + a_2[i-1]\mathbf{1}(-\epsilon_1-\epsilon_2)(-\epsilon_1-\epsilon_2) \\
&+ a_2[i+1]\mathbf{1}(\epsilon_1+\epsilon_2)(\epsilon_1+\epsilon_2) + a_1[i](\tau-\epsilon_1-\epsilon_2) + a_1[i+1](1-\tau+\epsilon_1+\epsilon_2) + \hat{n}_2[i], \qquad (24)
\end{aligned}
$$

where $\hat{n}_1[i] = \int_0^\infty n(t)p(t-iT-\epsilon_1 T)dt$ and $\hat{n}_2[i] = \int_0^\infty n(t)p(t-(i+\tau+\epsilon_1+\epsilon_2)T)dt$.

We note from (23) and (24) that the first sample vector is affected by the normalized synchronization timing error $\epsilon_1$ only, while the second sample vector is affected by the sum of the normalized synchronization timing error $\epsilon_1$ and the normalized coordination timing error $\epsilon_2$.

With (23) and (24), we obtain the outputs of the two matched filters at the BS subject to the timing error in the matrix form as

$$
\hat{\mathbf{Y}} = \hat{\mathbf{R}}\mathbf{H}\mathbf{X} + \hat{\mathbf{N}}, \qquad (25)
$$

where $\hat{\mathbf{Y}} = [\hat{y}_1[1]\ \hat{y}_2[1]\ \hat{y}_1[2]\ \hat{y}_2[2]\ \cdots\ \hat{y}_1[N]\ \hat{y}_2[N]]^T$, $\hat{\mathbf{N}} = [\hat{n}_1[1]\ \hat{n}_2[1]\ \hat{n}_1[2]\ \hat{n}_2[2]\ \cdots\ \hat{n}_1[N]\ \hat{n}_2[N]]^T$, and $\hat{\mathbf{R}}$ is given by

$$
\begin{aligned}
&\hat{\mathbf{R}} \\
&= \begin{bmatrix}
1-|\epsilon_1| & 1-\tau+\epsilon_1 & \mathbf{1}(\epsilon_1)\epsilon_1 & 0 & \cdots & \cdots & 0 \\
1-\tau-\epsilon_1-\epsilon_2 & 1-|\epsilon_1+\epsilon_2| & \tau+\epsilon_1+\epsilon_2 & \mathbf{1}(\epsilon_1+\epsilon_2)(\epsilon_1+\epsilon_2) & 0 & \cdots & 0 \\
\mathbf{1}(-\epsilon_1)(-\epsilon_1) & \tau-\epsilon_1 & 1-|\epsilon_1| & 1-\tau+\epsilon_1 & \mathbf{1}(\epsilon_1)\epsilon_1 & \cdots & 0 \\
\vdots & \ddots & \ddots & \ddots & \ddots & \ddots & \vdots \\
0 & \cdots & \mathbf{1}(-\epsilon_1-\epsilon_2)(-\epsilon_1-\epsilon_2) & 1-\tau-\epsilon_1-\epsilon_2 & 1-|\epsilon_1+\epsilon_2| & \tau+\epsilon_1+\epsilon_2 & \mathbf{1}(\epsilon_1+\epsilon_2)(\epsilon_1+\epsilon_2) \\
0 & \cdots & 0 & \mathbf{1}(-\epsilon_1)(-\epsilon_1) & \tau-\epsilon_1 & 1-|\epsilon_1| & 1-\tau+\epsilon_1 \\
0 & \cdots & \cdots & 0 & \mathbf{1}(-\epsilon_1-\epsilon_2)(-\epsilon_1-\epsilon_2) & 1-\tau-\epsilon_1-\epsilon_2 & 1-|\epsilon_1+\epsilon_2|
\end{bmatrix} \\
&= \mathbf{R}
\end{aligned}
$$

$$+\underbrace{\begin{bmatrix} -|\epsilon_1| & \epsilon_1 & \mathbf{1}(\epsilon_1)\epsilon_1 & 0 & \cdots & \cdots & 0 \\ -\epsilon_1-\epsilon_2 & -|\epsilon_1+\epsilon_2| & \epsilon_1+\epsilon_2 & \mathbf{1}(\epsilon_1+\epsilon_2)(\epsilon_1+\epsilon_2) & 0 & \cdots & 0 \\ \mathbf{1}(-\epsilon_1)(-\epsilon_1) & -\epsilon_1 & -|\epsilon_1| & \epsilon_1 & \mathbf{1}(\epsilon_1)\epsilon_1 & \cdots & 0 \\ \vdots & \ddots & \ddots & \ddots & \ddots & \ddots & \vdots \\ 0 & \cdots & \mathbf{1}(-\epsilon_1-\epsilon_2)(-\epsilon_1-\epsilon_2) & -\epsilon_1-\epsilon_2 & -|\epsilon_1+\epsilon_2| & \epsilon_1+\epsilon_2 & \mathbf{1}(\epsilon_1+\epsilon_2)(\epsilon_1+\epsilon_2) \\ 0 & \cdots & 0 & \mathbf{1}(-\epsilon_1)(-\epsilon_1) & -\epsilon_1 & -|\epsilon_1| & \epsilon_1 \\ 0 & \cdots & \cdots & 0 & \mathbf{1}(-\epsilon_1-\epsilon_2)(-\epsilon_1-\epsilon_2) & -\epsilon_1-\epsilon_2 & -|\epsilon_1+\epsilon_2| \end{bmatrix}}_{\mathbf{E}_1}. \tag{26}$$

We note from (26) that the expression for $\mathbf{E}_1$ is related to the signs of $\epsilon_1$ and $\epsilon_1+\epsilon_2$. For the sake of brevity, we present the analytical results for the case of $\epsilon_1 > 0$ and $\epsilon_1+\epsilon_2 > 0$ in the rest of the paper, while our analytical method and findings are applicable to all cases. In addition, we will present the numerical results in Section VI for all possible cases of $\epsilon_1$ and $\epsilon_1+\epsilon_2$. With $\epsilon_1 > 0$ and $\epsilon_1+\epsilon_2 > 0$, the expression for $\mathbf{E}_1$ is rewritten as

$$\mathbf{E}_1 = \epsilon_1 \underbrace{\begin{bmatrix} -1 & 1 & 1 & 0 & \cdots & \cdots & 0 \\ -1 & -1 & 1 & 1 & 0 & \cdots & 0 \\ 0 & -1 & -1 & 1 & 1 & \cdots & 0 \\ \vdots & \ddots & \ddots & \ddots & \ddots & \ddots & \vdots \\ 0 & \cdots & 0 & -1 & -1 & 1 & 1 \\ 0 & \cdots & 0 & 0 & -1 & -1 & 1 \\ 0 & \cdots & \cdots & 0 & 0 & -1 & -1 \end{bmatrix}}_{\mathbf{Z}_1} + \epsilon_2 \underbrace{\begin{bmatrix} 0 & 0 & 0 & 0 & \cdots & \cdots & 0 \\ -1 & -1 & 1 & 1 & 0 & \cdots & 0 \\ 0 & 0 & 0 & 0 & 0 & \cdots & 0 \\ \vdots & \ddots & \ddots & \ddots & \ddots & \ddots & \vdots \\ 0 & \cdots & 0 & -1 & -1 & 1 & 1 \\ 0 & \cdots & 0 & 0 & 0 & 0 & 0 \\ 0 & \cdots & \cdots & 0 & 0 & -1 & -1 \end{bmatrix}}_{\mathbf{Z}_2}. \tag{27}$$

The covariance matrix of $\hat{\mathbf{N}}$ is given by

$$\begin{aligned} \hat{\mathbf{R}}_{\mathbf{N}} = \mathbb{E}\left\{\hat{\mathbf{N}}\hat{\mathbf{N}}^H\right\} &= \begin{bmatrix} 1 & 1-\tau-\epsilon_2 & 0 & \cdots & \cdots & 0 \\ 1-\tau-\epsilon_2 & 1 & \tau+\epsilon_2 & 0 & \cdots & 0 \\ 0 & \tau+\epsilon_2 & 1 & 1-\tau-\epsilon_2 & \cdots & 0 \\ \vdots & \ddots & \ddots & \ddots & \ddots & \vdots \\ 0 & \cdots & 0 & \tau+\epsilon_2 & 1 & 1-\tau-\epsilon_2 \\ 0 & \cdots & \cdots & 0 & 1-\tau-\epsilon_2 & 1 \end{bmatrix} \\ &= \mathbf{R} + \underbrace{\begin{bmatrix} 0 & -\epsilon_2 & 0 & \cdots & \cdots & 0 \\ -\epsilon_2 & 0 & \epsilon_2 & 0 & \cdots & 0 \\ 0 & \epsilon_2 & 0 & -\epsilon_2 & \cdots & 0 \\ \vdots & \ddots & \ddots & \ddots & \ddots & \vdots \\ 0 & \cdots & 0 & \epsilon_2 & 0 & -\epsilon_2 \\ 0 & \cdots & \cdots & 0 & -\epsilon_2 & 0 \end{bmatrix}}_{\mathbf{E}_2}, \end{aligned} \tag{28}$$

where $\mathbf{E}_2$ can be rewritten as

$$\mathbf{E}_2 = \epsilon_2 \underbrace{\begin{bmatrix} 0 & -1 & 0 & \cdots & \cdots & 0 \\ -1 & 0 & 1 & 0 & \cdots & 0 \\ 0 & 1 & 0 & -1 & \cdots & 0 \\ \vdots & \ddots & \ddots & \ddots & \ddots & \vdots \\ 0 & \cdots & 0 & 1 & 0 & -1 \\ 0 & \cdots & \cdots & 0 & -1 & 0 \end{bmatrix}}_{\mathbf{Z}_3}. \tag{29}$$

We note from (29) that the covariance matrix of the noise terms is affected by the normalized coordination timing error $\epsilon_2$, while it is not related to the normalized synchronization timing error $\epsilon_1$.

### C. Impact of Timing Error on Throughput Performance

According to (25), the throughput of the ANOMA system with timing error is given by

$$\begin{aligned}
&R_e^{\mathrm{ANOMA}} \\
&= \frac{1}{N+\tau}\log\det\left(\mathbf{I}_{2N}+\hat{\mathbf{R}}_{\mathbf{N}}^{-1}\hat{\mathbf{R}}\mathbf{H}\mathbf{H}^H\hat{\mathbf{R}}^H\right) \\
&= \frac{1}{N+\tau}\log\det\left(\mathbf{I}_{2N}+(\mathbf{R}+\mathbf{E}_2)^{-1}(\mathbf{R}+\mathbf{E}_1)\mathbf{H}\mathbf{H}^H(\mathbf{R}+\mathbf{E}_1^H)\right) \\
&= \frac{1}{N+\tau}\log\det\left(\mathbf{I}_{2N}+\left(\mathbf{I}_{2N}+(\mathbf{R}+\mathbf{E}_2)^{-1}(\mathbf{E}_1-\mathbf{E}_2)\right)\mathbf{H}\mathbf{H}^H(\mathbf{R}+\mathbf{E}_1^H)\right) \\
&= \frac{1}{N+\tau}\log\det\left(\mathbf{I}_{2N}+\mathbf{H}\mathbf{H}^H\mathbf{R}+\mathbf{H}\mathbf{H}^H\mathbf{E}_1^H+(\mathbf{R}+\mathbf{E}_2)^{-1}(\mathbf{E}_1-\mathbf{E}_2)\mathbf{H}\mathbf{H}^H(\mathbf{R}+\mathbf{E}_1^H)\right). \quad (30)
\end{aligned}$$

When there is no timing error, i.e., $\epsilon_1=\epsilon_2=0$, we have $\mathbf{E}_1=\mathbf{E}_2=\mathbf{0}$. Hence, substituting $\mathbf{E}_1=\mathbf{E}_2=\mathbf{0}$ into (30), we obtain the throughput of the ANOMA system without timing error, which is the same as (14).

From (14) and (30), we derive the throughput loss incurred by the timing error as

$$\begin{aligned}
\Delta &= R^{\mathrm{ANOMA}} - R_e^{\mathrm{ANOMA}} \\
&= -\frac{1}{N+\tau}\log\det\Big\{\mathbf{I}_{2N}+\left(\mathbf{I}_{2N}+\mathbf{H}\mathbf{H}^H\mathbf{R}\right)^{-1}\big[\mathbf{H}\mathbf{H}^H\mathbf{E}_1^H \\
&\quad +(\mathbf{R}+\mathbf{E}_2)^{-1}(\mathbf{E}_1-\mathbf{E}_2)\mathbf{H}\mathbf{H}^H(\mathbf{R}+\mathbf{E}_1^H)\big]\Big\}. \quad (31)
\end{aligned}$$

In what follows, we separately analyze the throughput loss incurred by the synchronization timing error and the coordination timing error with the practical consideration that these two types of timing error both are relatively small.

*1) Impact of Synchronization Timing Error:* We first investigate the impact of synchronization timing error on the throughput loss and consider the practical scenario where the error is relatively small, such that $\epsilon_2=0$ and $\epsilon_1\ll 1$.

In this case, by omitting high-order terms of $\epsilon_1$, we obtain the throughput loss incurred by the synchronization timing error from (31) as

$$\begin{aligned}
\Delta_{\epsilon_1} &= -\frac{1}{N+\tau}\log\det\Big\{\mathbf{I}_{2N}+\epsilon_1\left(\mathbf{I}_{2N}+\mathbf{H}\mathbf{H}^H\mathbf{R}\right)^{-1}\left[\mathbf{H}\mathbf{H}^H\mathbf{Z}_1^H+\mathbf{R}^{-1}\mathbf{Z}_1\mathbf{H}\mathbf{H}^H(\mathbf{R}+\epsilon_1\mathbf{Z}_1^H)\right]\Big\} \\
&\overset{(a)}{\approx} -\frac{1}{N+\tau}\log\det\Big\{\mathbf{I}_{2N}+\epsilon_1\left(\mathbf{I}_{2N}+\mathbf{H}\mathbf{H}^H\mathbf{R}\right)^{-1}\left[\mathbf{H}\mathbf{H}^H\mathbf{Z}_1^H+\mathbf{R}^{-1}\mathbf{Z}_1\mathbf{H}\mathbf{H}^H\mathbf{R}\right]\Big\} \\
&\overset{(b)}{\approx} -\frac{1}{N+\tau}\log\left(1+\epsilon_1\mathrm{Tr}(\mathbf{F}_1)+O(\epsilon_1^2)\right) \overset{(c)}{\approx} \epsilon_1 c_1, \quad (32)
\end{aligned}$$

where $\mathbf{F}_1 = \left(\mathbf{I}_{2N} + \mathbf{H}\mathbf{H}^H\mathbf{R}\right)^{-1}\left(\mathbf{H}\mathbf{H}^H\mathbf{Z}_1^H + \mathbf{R}^{-1}\mathbf{Z}_1\mathbf{H}\mathbf{H}^H\mathbf{R}\right)$, $c_1 = -\frac{1}{N+\tau}\mathrm{Tr}(\mathbf{F}_1)$, $(a)$ is approximated by using $\mathbf{R} + \epsilon_1\mathbf{Z} \approx \mathbf{R}$ as $\epsilon_1 \to 0$, $(b)$ is derived using the special case of Jacobi's formula [25], i.e., $\det(\mathbf{I} + \epsilon\mathbf{A}) = 1 + \epsilon\mathrm{Tr}(\mathbf{A}) + O(\epsilon^2)$, and $(c)$ is derived by omitting the high-order terms of $\epsilon_1$ and applying the approximation $\log(1+x) \approx x$ when $x \ll 1$. From (32), we note that the throughput loss is approximately linear to $\epsilon_1$ when $\epsilon_2 = 0$ and $\epsilon_1 \ll 1$.

*2) Impact of Coordination Timing Error:* We now investigate the impact of the coordination timing error on the throughput loss and still consider the practical scenario where the error is relatively small, such that $\epsilon_1 = 0$ and $\epsilon_2 \ll 1$.

By omitting high-order terms of $\epsilon_2$, we obtain the throughput loss incurred by the coordination timing error from (31) as

$$\Delta_{\epsilon_2} = -\frac{1}{N+\tau}\log\det\Big\{\mathbf{I}_{2N} + \epsilon_2\left(\mathbf{I}_{2N} + \mathbf{H}\mathbf{H}^H\mathbf{R}\right)^{-1}\big[\mathbf{H}\mathbf{H}^H\mathbf{Z}_2^H + (\mathbf{R} + \epsilon_2\mathbf{Z}_3)^{-1}(\mathbf{Z}_2 - \mathbf{Z}_3)\mathbf{H}\mathbf{H}^H(\mathbf{R} + \epsilon_2\mathbf{Z}_2^H)\big]\Big\} \overset{(a)}{\approx} \epsilon_2 c_2, \tag{33}$$

where $\mathbf{F}_2 = \left(\mathbf{I}_{2N} + \mathbf{H}\mathbf{H}^H\mathbf{R}\right)^{-1}\left(\mathbf{H}\mathbf{H}^H\mathbf{Z}_2^H + \mathbf{R}^{-1}(\mathbf{Z}_2 - \mathbf{Z}_3)\mathbf{H}\mathbf{H}^H\mathbf{R}\right)$, $c_2 = -\frac{1}{N+\tau}\mathrm{Tr}(\mathbf{F}_2)$, and $(a)$ can be derived by following the same steps in the derivation of (32). From (33), we note that the throughput loss is approximately linear to $\epsilon_2$ when $\epsilon_1 = 0$ and $\epsilon_2 \ll 1$.

## VI. Numerical Results

In this section, we present numerical results to compare the throughput performances of NOMA and ANOMA systems and illustrate the impact of timing error on the performance of the ANOMA system. Figures 5, 6, and 7 show the ANOMA system without timing error while the other figures are for the impact of timing error. In our simulations, we set the symbol length $T = 1$ and the AWGN with unit power. If not specified, the normalized timing mismatch between the two signals $\tau$ is set to 0.5.

At first, we present the throughput performances of NOMA and ANOMA systems under different channel conditions and pulse shapes in Figure 4. In Fig. 4, the curves of "ANOMA in (14)" are derived directly from the definition in (14), and the curves of "ANOMA in (16)" are obtained from our result in Theorem 1. Note that the performance of NOMA is not affected by the adopted pulse shape if the pulse shape has unit power and causes no inter-symbol interference. It is shown that, for the rectangular pulse shape, the throughput computed by Theorem 1 completely aligns with that calculated by (14) for different combinations of channel conditions, which confirms the correctness of Theorem 1. Besides, Fig. 4 demonstrates that the throughputs of

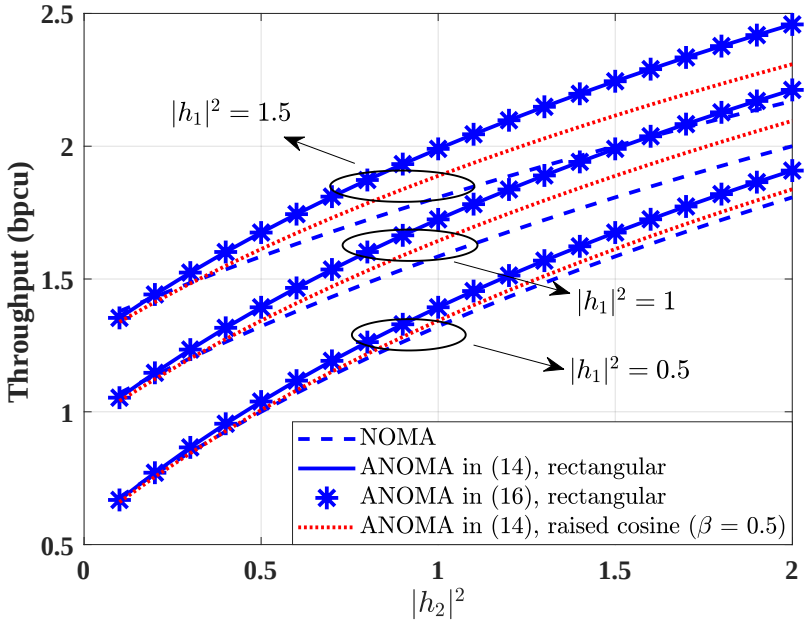


Fig. 4: The sum throughput of two users as a function of channel gains for ANOMA and NOMA systems when $P_1 = 1$, $P_2 = 1$, $\tau = 0.5$, and $N = 10$.

ANOMA and NOMA systems increase with the channel gains $|h_1|^2$ and $|h_2|^2$ for both rectangular and raised cosine pulse shapes. Furthermore, the ANOMA systems using the rectangular pulse shape outperform those using the raised cosine pulse shape with roll-off factor $\beta = 0.5$. It is because the raised cosine pulse shape spans more than one symbol time, causing more severe interference compared with the rectangular pulse shape.

Then, we compare the throughput performances of NOMA and ANOMA systems. Figure 5 shows the throughput as a function of the frame length $N$. In Fig. 5, it is demonstrated that as $N$ increases, the throughput of ANOMA systems converges to the result in Corollary 1, which provides the throughput in the asymptotic case of $N \to \infty$. Furthermore, we note from the figure that the throughputs of ANOMA systems for different $\tau$s as $N \to \infty$ are greater than that of the NOMA system, which is consistent with our analytical results in Theorem 2 and Corollary 2. In global system for mobile communications (GSM), there are approximately 156 symbols in a normal burst (a physical channel carrying information on traffic and control channels) [26]. In LTE, there are 140 symbols with normal cyclic prefix (CP) in a frame [22]. We find from Fig. 5 that the ANOMA outperforms the NOMA if $N$ is greater than 20, which is much smaller than the number of symbols in a burst/frame of GSM/LTE. Since the needed frame length of ANOMA to outperform NOMA is much less than the burst/frame length in GSM/LTE systems,

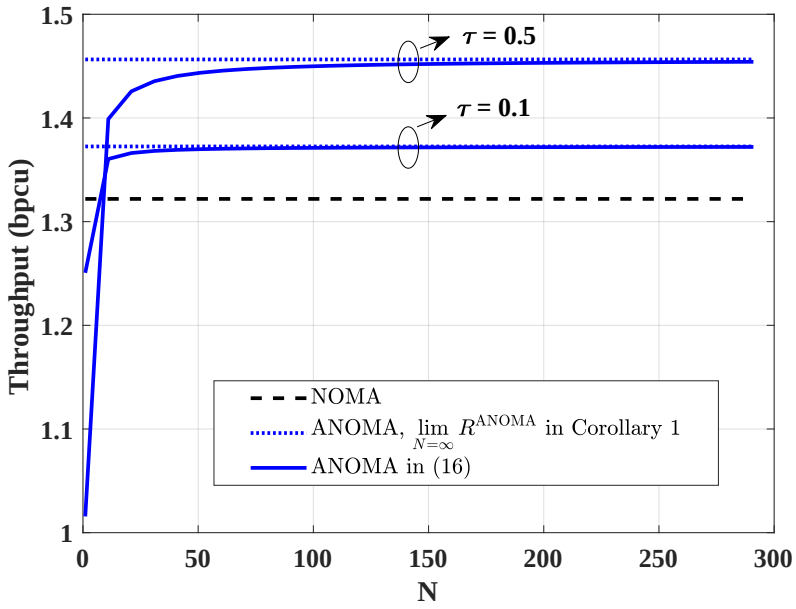


Fig. 5: The sum throughput of two users as a function of the frame length $N$ for ANOMA and NOMA systems when $P_1|h_1|^2 = 1$, $P_2|h_2|^2 = 0.5$, $\tau = 0.5$ or 0.1.

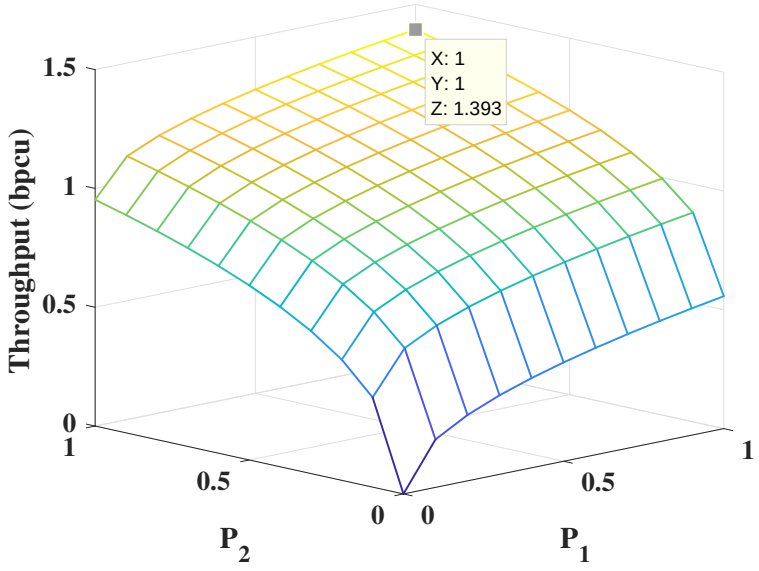


Fig. 6: The sum throughput of two users as a function of transmit powers of Users 1 & 2 for ANOMA systems when $|h_1|^2 = 1$, $|h_2|^2 = 0.5$, $P_{1,\max} = P_{2,\max} = 1$, $\tau = 0.5$, and $N = 10$.

the detection delay is within a reasonable range.

In addition, we illustrate the optimal parameter design of the ANOMA system in Figures 6 and 7. Figure 6 demonstrates the sum throughput of two users as a function of their transmit

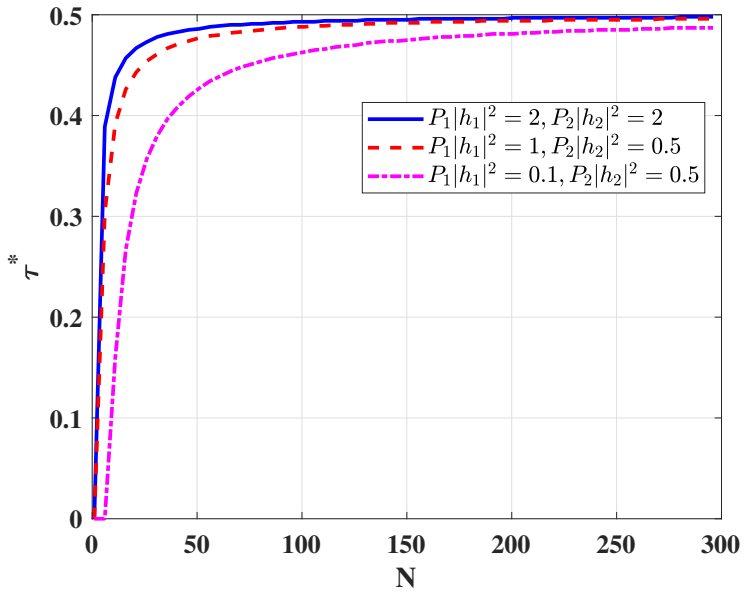


Fig. 7: The optimal normalized timing mismatch $\tau^*$ to maximize the sum throughput of two users as a function of the frame length $N$ for different channel conditions.

powers. It is shown that the maximal sum throughput is reached when the transmit powers are equal to the maximum available powers, which aligns with Theorem 3. We present the optimal normalized timing mismatch $\tau^*$ found by exhaustive search to maximize the sum throughput of two users in Figure 7. As shown in Fig. 7, $\tau^*$ starts with 0, and then increases with $N$, finally converges to 0.5 as $N$ grows, which verifies the correctness of Theorem 4.

Figure 5 demonstrates that ANOMA outperforms NOMA for $N \geq 20$ in the considered scenario. Also, from Fig. 7, we note that the optimal $\tau$ closely approaches 0.5 as $N \geq 50$. It is worth mentioning that having $N \geq 50$ is reasonable for practical communication systems. For a high-speed train traveling at 200 km/h using a 900 MHz carrier, the coherence time is approximately 3 ms [26]. In GSM (operating at 900 MHz), the symbol rate is approximately 271 ksymbols/second. As a result, it is reasonable to assume a static channel with flat fading if the frame length $N$ does not exceed 3 ms $\times$ 271 ksymbols/second = 813, which is much greater than the threshold needed, i.e., 50.

In what follows, we evaluate the impact of timing error on the throughput of ANOMA systems. In the following figures, the throughput loss ratio is defined as the ratio of the throughput loss in (31) and the throughput of the ANOMA system without timing error in (14), i.e.,$\gamma = \frac{\Delta}{R^{\text{ANOMA}}}$.

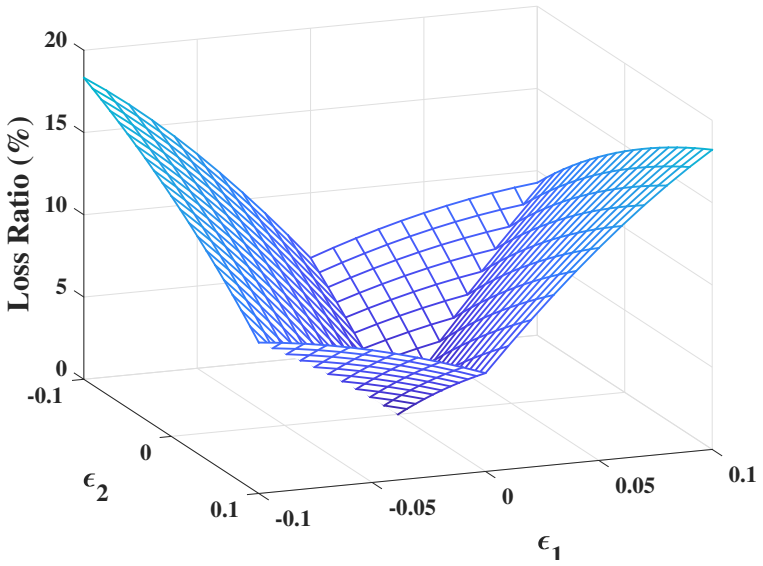


Fig. 8: The throughput loss ratio as a function of the normalized synchronization timing error $\epsilon_1$ and the normalized coordination timing error $\epsilon_2$ when $P_1|h_1|^2 = 1$, $P_2|h_2|^2 = 0.5$, $\tau = 0.5$ and $N = 10$.

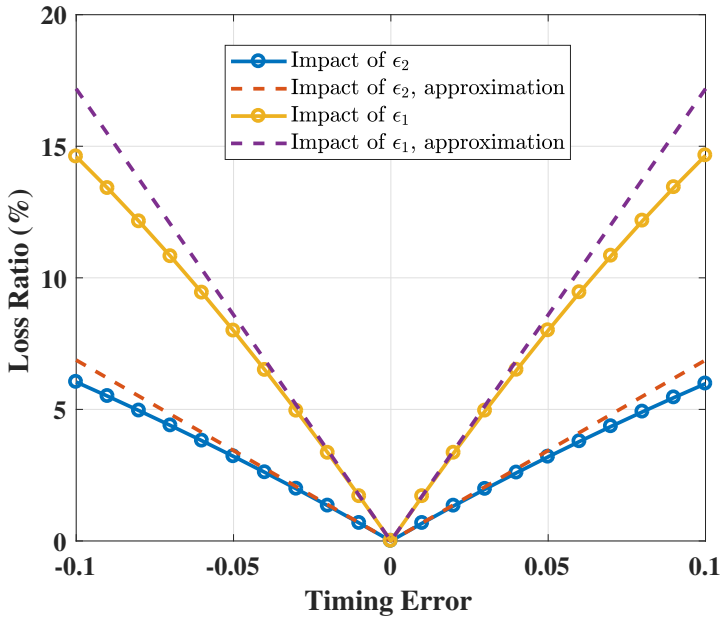


Fig. 9: The individual impacts of the normalized synchronization timing error $\epsilon_1$ and the normalized coordination timing error $\epsilon_2$ on the throughput loss ratio when $P_1|h_1|^2 = 1$, $P_2|h_2|^2 = 0.5$, $\tau = 0.5$, and $N = 10$.

In Fig. 8, we present the throughput loss ratio as a function of $\epsilon_1$ and $\epsilon_2$ ranging from -0.1 to 0.1. As shown in Fig. 8, the throughput loss ratio increases with both the synchronization timing error and the coordination timing error. We also find that the throughput loss ratio $\gamma$ is a

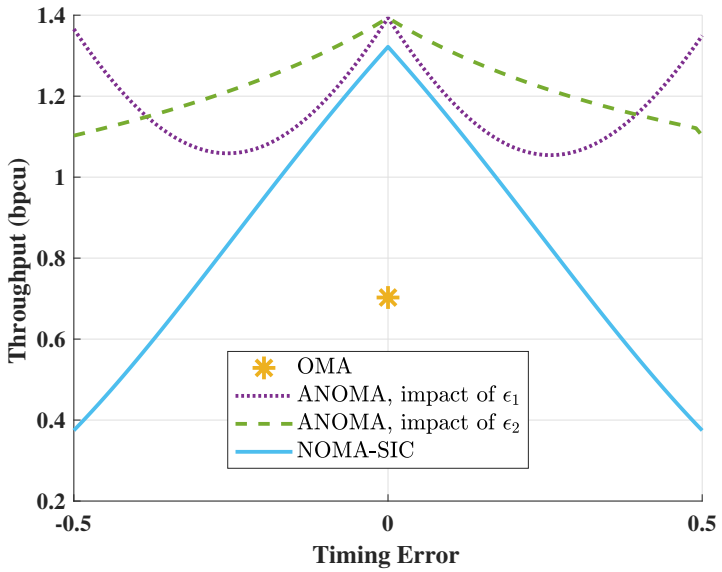


Fig. 10: Comparison of throughputs among OMA, NOMA, and ANOMA when $P_1|h_1|^2 = 1$, $P_2|h_2|^2 = 0.5$, $\tau = 0.5$, and $N = 10$.

continuous function with respect to $\epsilon_1$ and $\epsilon_2$ but non-differentiable when $\epsilon_1 = 0$ or $\epsilon_1 + \epsilon_2 = 0$. This is because there are non-linear step functions in the expression for $\mathbf{E}_1$ in (26). We find from the figure that there still exists a considerable performance loss when $\epsilon_1 + \epsilon_2 = 0$, which can be explained as follows. Note that $\epsilon_1 + \epsilon_2 = 0$ does not necessarily mean that $\epsilon_1 = 0$ and $\epsilon_2 = 0$, since $\epsilon_1$ and $\epsilon_2$ can be negative values. The system may be still affected by non-zero timing errors, even when $\epsilon_1 + \epsilon_2 = 0$. According to (23) and (24), when $\epsilon_1 + \epsilon_2 = 0$, the first sample vector is still affected by $\epsilon_1$, although the second sample vector will have no timing error.

We also study the individual effects of the timing synchronization error and the coordination timing error on the throughput of ANOMA systems. In Fig. 9, we show the throughput loss ratio as a function of $\epsilon_1$ when $\epsilon_2 = 0$ and $\epsilon_2$ when $\epsilon_1 = 0$. Note that the curves of "impact of $\epsilon_1$" and "impact of $\epsilon_2$" are the slices of Fig. 8 when $\epsilon_2 = 0$ and $\epsilon_1 = 0$, respectively. The approximated results are calculated by $\Delta_{\epsilon_1}/R^{\mathrm{ANOMA}}$ and $\Delta_{\epsilon_2}/R^{\mathrm{ANOMA}}$ using (32) and (33). It is demonstrated that the expressions in (32) and (33) are good approximations of (31) when $|\epsilon_1| < 0.05$ and $|\epsilon_2| < 0.05$, respectively. Besides, $\epsilon_1$ causes almost twice throughput loss compared with $\epsilon_2$ for the same value of error. This phenomenon reveals that the synchronization timing error deteriorates the system performance more severely compared with the coordination timing error. This observation can be explained as follows. With the oversampling, the sampling instants are

at $(i+\epsilon_1)T$ and $(i+\tau+\epsilon_1+\epsilon_2)T$, $i=1,\cdots,N$, which illustrates that the synchronization timing error affects all sampling instants while the coordination timing error only has impacts on half of the sampling instants.

Finally, we compare the performances of OMA, NOMA, ANOMA without and with timing error in Figure 10. In our simulation, the conventional TDMA is adopted as the OMA scheme. As shown in the figure, the throughput curve of OMA is a single point because it is not a function of timing error. The throughput of the NOMA system is calculated under the assumption that perfect SIC is realized at BS. It is demonstrated that the rate performance for ANOMA without timing error is better than that of NOMA with SIC which is further greater than that of OMA. Also, ANOMA always outperforms a perfectly synchronized OMA. We note that for small values of timing error, ANOMA outperforms even a perfectly synchronized NOMA. For the same timing error, the performance of ANOMA is better than that of NOMA. Besides, as shown in Fig. 10, the throughput decreases with the absolute value of $\epsilon_2$ monotonously, while the throughput decreases at the beginning and then increases as the absolute value of $\epsilon_1$ increases. This phenomenon can be explained as follows: If there is no timing error ($\epsilon_1=\epsilon_2=0$) and $\tau=0.5$, the sampling moments are at $iT$ and $(i+0.5)T$, $i=1,\cdots,N$. If $|\epsilon_1|=0.5$ and $\epsilon_2=0$, the sampling moments are at $(i\pm0.5)T$ and $(i+1\pm0.5)T$, $i=1,\cdots,N$, which are equivalent to advancing ($\epsilon_1=-0.5$) or delaying ($\epsilon_1=0.5$) all sampling moments by $0.5T$. The sampling diversity can still be achieved except that there will be throughput loss due to the shift of sampling moments. For the case $\epsilon_1=0$ and $|\epsilon_2|=0.5$, the second sample vector is a duplicate ($\epsilon_2=-0.5$) or shifted version ($\epsilon_2=0.5$) of the first sample vector. Hence, the sampling diversity cannot be obtained and only the first sample vector can be used to recover the transmitted symbols.

## VII. Conclusion and Future Work

In this paper, we have studied the performance of a two-user uplink ANOMA system and compared it with the NOMA system. We derive an analytical expression for the two-user sum throughput in the ANOMA system as a function of SNR, frame length, and normalized timing mismatch. We have demonstrated that the ANOMA outperforms the NOMA when the frame length is sufficiently large. Furthermore, we have shown that two users should transmit at full power to maximize the two-user sum throughput. The optimal timing mismatch to maximize the sum throughput converges to a half of one time slot as the frame length goes to infinity. Besides,

we discuss the impact of timing error on the throughput performance of the ANOMA system, including the synchronization timing error and the coordination timing error. We have shown how these two types of timing error individually and jointly affect the throughput performance of the ANOMA system.

As an initial comprehensive study on uplink ANOMA systems, our paper can lead to a number of future research directions in this area. While this paper has considered only 2 users, the ANOMA scheme can be extended to the multi-user (more than 2 users) scenario. In a $K$-user scenario, the BS should use $K$ samples per symbol length, each aligned with one of the users to obtain sampling diversity. The study of ANOMA in a more than two-user scenario is an interesting future work. It is also an interesting problem to study the ANOMA in a multicell scenario. Besides, it is worthwhile extending the considered ANOMA in this paper into the OFDM systems, since current wireless communication systems are often based on the OFDM technique. For OFDM systems, one can introduce the frequency-domain asynchrony instead of the time-domain asynchrony and apply similar ideas presented in this paper to design ANOMA OFDM schemes. Moreover, a further analysis on the bit error rate performance of the ANOMA systems can be a good future work.

## ACKNOWLEDGEMENT

The authors would like to thank Mehdi Ganji for insightful conversation regarding timing error.

## APPENDIX A
## PROOF OF THEOREM 1

*Proof:* According to (14), we can rewrite $\det\left(\mathbf{I}_{2N}+\mathbf{H}\mathbf{H}^H\mathbf{R}\right)$ as

$$\begin{aligned}\det\left(\mathbf{I}_{2N}+\mathbf{H}\mathbf{H}^H\mathbf{R}\right) &= \det\left(\mathbf{H}\mathbf{H}^H\right)\det\left((\mathbf{H}\mathbf{H}^H)^{-1}+\mathbf{R}\right)\\ &= \left(P_1|h_1|^2\right)^N\left(P_2|h_2|^2\right)^N\det\left((\mathbf{H}\mathbf{H}^H)^{-1}+\mathbf{R}\right). \end{aligned} \tag{34}$$

According to (8) and (9), $(\mathbf{H}\mathbf{H}^H)^{-1}+\mathbf{R}$ is a $2N\times 2N$ matrix calculated by

$$(\mathbf{H}\mathbf{H}^H)^{-1}+\mathbf{R}=\begin{bmatrix} 1+\left(P_1|h_1|^2\right)^{-1} & 1-\tau & 0 & \cdots & \cdots & 0\\ 1-\tau & 1+\left(P_2|h_2|^2\right)^{-1} & \tau & 0 & \cdots & 0\\ \vdots & \ddots & \ddots & \ddots & \ddots & \vdots\\ 0 & \cdots & 1-\tau & 1+\left(P_2|h_2|^2\right)^{-1} & \tau & 0\\ 0 & \cdots & 0 & \tau & 1+\left(P_1|h_1|^2\right)^{-1} & 1-\tau\\ 0 & \cdots & \cdots & 0 & 1-\tau & 1+\left(P_2|h_2|^2\right)^{-1} \end{bmatrix}. \tag{35}$$

For simplicity of presentation, we define $\mu_1 = P_1|h_1|^2$, $\mu_2 = P_2|h_2|^2$, and

$$d_m = \begin{cases} \det\left(\begin{bmatrix} 1+\mu_1^{-1} & 1-\tau & 0 & \cdots & \cdots & 0 \\ 1-\tau & 1+\mu_2^{-1} & \tau & 0 & \cdots & 0 \\ \vdots & \ddots & \ddots & \ddots & \ddots & \vdots \\ 0 & \cdots & 1-\tau & 1+\mu_2^{-1} & \tau & 0 \\ 0 & \cdots & 0 & \tau & 1+\mu_1^{-1} & 1-\tau \\ 0 & \cdots & \cdots & 0 & 1-\tau & 1+\mu_2^{-1} \end{bmatrix}_{m\times m}\right), & \text{if } m \text{ is even}, \\ \det\left(\begin{bmatrix} 1+\mu_1^{-1} & 0 & 1-\tau & \cdots & \cdots & 0 \\ 1-\tau & 1+\mu_2^{-1} & \tau & 0 & \cdots & 0 \\ \vdots & \ddots & \ddots & \ddots & \ddots & \vdots \\ 0 & \cdots & \tau & 1+\mu_1^{-1} & 1-\tau & 0 \\ 0 & \cdots & 0 & 1-\tau & 1+\mu_2^{-1} & \tau \\ 0 & \cdots & \cdots & 0 & \tau & 1+\mu_1^{-1} \end{bmatrix}_{m\times m}\right), & \text{if } m \text{ is odd}. \end{cases} \tag{36}$$

Thus, $\det\left((\mathbf{H}\mathbf{H}^H)^{-1} + \mathbf{R}\right) = d_{2N}$.

By the method of cofactor expansion [27], the determinant of $\det\left((\mathbf{H}\mathbf{H}^H)^{-1} + \mathbf{R}\right)$ can be expressed as a weighted sum of the determinants of its minors. The minor $M_{i,j}$ is defined as the determinant of the matrix that results from $(\mathbf{H}\mathbf{H}^H)^{-1} + \mathbf{R}$ by removing the $i$th row and the $j$th column. Then, we have

$$\begin{aligned} d_{2N} &= \sum_{j=1}^{2N} (-1)^{2N+j} a_{2N,j} M_{2N,j} \\ &= (-1)^{2N+2N}\left(1+\mu_2^{-1}\right) \underbrace{\det\left(\begin{bmatrix} 1+\mu_1^{-1} & 1-\tau & \cdots & \cdots & 0 \\ 1-\tau & 1+\mu_2^{-1} & \tau & \cdots & 0 \\ \vdots & \ddots & \ddots & \ddots & \vdots \\ 0 & \cdots & 1-\tau & 1+\mu_2^{-1} & \tau \\ 0 & \cdots & 0 & \tau & 1+\mu_1^{-1} \end{bmatrix}_{(2N-1)\times(2N-1)}\right)}_{d_{2N-1}} \\ &\quad + (-1)^{2N+2N-1}(1-\tau)\det\left(\begin{bmatrix} 1+\mu_1^{-1} & 1-\tau & \cdots & \cdots & 0 \\ 1-\tau & 1+\mu_2^{-1} & \tau & \cdots & 0 \\ \vdots & \ddots & \ddots & \ddots & \vdots \\ 0 & \cdots & 1-\tau & 1+\mu_2^{-1} & 0 \\ 0 & \cdots & 0 & \tau & 1-\tau \end{bmatrix}_{(2N-1)\times(2N-1)}\right) \\ &= \left(1+\mu_2^{-1}\right) d_{2N-1} \\ &\quad - (1-\tau)^2(-1)^{4N-2} \underbrace{\det\left(\begin{bmatrix} 1+\mu_1^{-1} & 1-\tau & 0 & \cdots & \cdots & 0 \\ 1-\tau & 1+\mu_2^{-1} & \tau & 0 & \cdots & 0 \\ \vdots & \ddots & \ddots & \ddots & \ddots & \vdots \\ 0 & \cdots & 1-\tau & 1+\mu_2^{-1} & \tau & 0 \\ 0 & \cdots & 0 & \tau & 1+\mu_1^{-1} & 1-\tau \\ 0 & \cdots & \cdots & 0 & 1-\tau & 1+\mu_2^{-1} \end{bmatrix}_{(2N-2)\times(2N-2)}\right)}_{d_{2N-2}} \\ &= \left(1+\mu_2^{-1}\right) d_{2N-1} - (1-\tau)^2 d_{2N-2}, \end{aligned} \tag{37}$$

where $N \geq 2$ and $a_{i,j}$ denotes the element of the matrix $(\mathbf{H}\mathbf{H}^H)^{-1} + \mathbf{R}$ at the $i$th row and the $j$th column. Similarly, we can also write the recursive formula for $d_{2N-1}$ as

$$d_{2N-1} = (1 + \mu_1^{-1})d_{2N-2} - \tau^2 d_{2N-3}. \tag{38}$$

From (37) and (38), we obtain

$$d_{2N} = \left[\mu_1^{-1} + \mu_2^{-1} + \mu_1^{-1}\mu_2^{-1} + 2\tau(1-\tau)\right] d_{2N-2} - \tau^2(1-\tau)^2 d_{2N-4}. \tag{39}$$

To formalize (39) as the recursion formula of a geometric progression, (39) can be rewritten as

$$d_{2N} - r_1 d_{2N-2} = r_2(d_{2N-2} - r_1 d_{2N-4}), \tag{40}$$

$$d_{2N} - r_2 d_{2N-2} = r_1(d_{2N-2} - r_2 d_{2N-4}), \tag{41}$$

where

$$r_1 = \frac{\mu_1^{-1}+\mu_2^{-1}+\mu_1^{-1}\mu_2^{-1}+2\tau(1-\tau)+\sqrt{\left[\mu_1^{-1} + \mu_2^{-1} + \mu_1^{-1}\mu_2^{-1} + 2\tau(1-\tau)\right]^2-4\tau^2(1-\tau)^2}}{2}, \tag{42}$$

$$r_2 = \frac{\mu_1^{-1}+\mu_2^{-1}+\mu_1^{-1}\mu_2^{-1}+2\tau(1-\tau)-\sqrt{\left[\mu_1^{-1} + \mu_2^{-1} + \mu_1^{-1}\mu_2^{-1} + 2\tau(1-\tau)\right]^2-4\tau^2(1-\tau)^2}}{2}. \tag{43}$$

Since $\mu_1 > 0$, $\mu_2 > 0$, and $\tau \in [0, 1)$, we note that the part under the square root symbol in (42) and (43) is always positive, such that

$$\begin{aligned}&\left[\mu_1^{-1} + \mu_2^{-1} + \mu_1^{-1}\mu_2^{-1} + 2\tau(1-\tau)\right]^2 - 4\tau^2(1-\tau)^2 \\ &= \left[\mu_1^{-1} + \mu_2^{-1} + \mu_1^{-1}\mu_2^{-1} + 4\tau(1-\tau)\right]\left[\mu_1^{-1} + \mu_2^{-1} + \mu_1^{-1}\mu_2^{-1}\right] > 0.\end{aligned} \tag{44}$$

From (40) and (41), we obtain

$$d_{2N} - r_1 d_{2N-2} = r_2^{N-1}(d_2 - r_1 d_0), \tag{45}$$

$$d_{2N} - r_2 d_{2N-2} = r_1^{N-1}(d_2 - r_2 d_0). \tag{46}$$

Solving $d_{2N}$ from the equation group constituted by (45) and (46), we derive

$$d_{2N} = \frac{r_1^N(d_2 - r_2 d_0) - r_2^N(d_2 - r_1 d_0)}{r_1 - r_2}. \tag{47}$$

Substituting $d_0 = 1$ and

$$d_2 = \begin{bmatrix} 1 + \mu_1^{-1} & 1 - \tau \\ 1 - \tau & 1 + \mu_2^{-1} \end{bmatrix} = \left(1 + \mu_1^{-1}\right)\left(1 + \mu_2^{-1}\right) - (1-\tau)^2 = r_1 + r_2 + \tau^2 \tag{48}$$

into (47), we have

$$d_{2N} = \frac{(r_1^{N+1} - r_2^{N+1}) + \tau^2(r_1^N - r_2^N)}{r_1 - r_2}. \tag{49}$$

Finally, based on (34) and (49), we obtain the throughput as

$$R^{\mathrm{ANOMA}} = \frac{N}{N+\tau}\log\left(\mu_1\mu_2\right) + \frac{1}{N+\tau}\log\frac{(r_1^{N+1} - r_2^{N+1}) + \tau^2(r_1^N - r_2^N)}{r_1 - r_2}. \tag{50}$$

This completes the proof. ■

## APPENDIX B
## PROOF OF COROLLARY 1

*Proof:* Note that $\mu_1$, $\mu_2$, $r_1$, $r_2$, and $\tau$ are all independent of $N$. We then have

$$\begin{aligned}
\lim_{N\to\infty} R^{\mathrm{ANOMA}} &= \lim_{N\to\infty} \frac{N}{N+\tau}\log(\mu_1\mu_2) + \frac{\log\left[(r_1^{N+1} - r_2^{N+1}) + \tau^2(r_1^N - r_2^N)\right] - \log(r_1 - r_2)}{N+\tau} \\
&\overset{(a)}{=} \log(\mu_1\mu_2) + \lim_{N\to\infty} \frac{(r_1^{N+1}\log r_1 - r_2^{N+1}\log r_2) + \tau^2(r_1^N\log r_1 - r_2^N\log r_2)}{(r_1^{N+1} - r_2^{N+1}) + \tau^2(r_1^N - r_2^N)} \\
&\overset{(b)}{=} \log(\mu_1\mu_2) + \lim_{N\to\infty} \frac{(r_1\alpha^N\log r_1 - r_2\log r_2) + \tau^2(\alpha^N\log r_1 - \log r_2)}{(r_1\alpha^N - r_2) + \tau^2(\alpha^N - 1)} \\
&= \log(\mu_1\mu_2) + \lim_{N\to\infty} \frac{\alpha^N(r_1+\tau^2)\log r_1 - (r_2+\tau^2)\log r_2}{\alpha^N(r_1+\tau^2) - (r_2+\tau^2)} \\
&\overset{(c)}{=} \log\left(\mu_1\mu_2 r_1\right),
\end{aligned} \tag{51}$$

where $\alpha = r_1/r_2$, $(a)$ is derived by applying L'Hospital's rule, $(b)$ is derived by dividing both the numerator and the denominator by $r_2^N$, and $(c)$ is obtained from the facts that $r_1 > r_2 > 0$ and $\alpha > 1$ according to (17) and (18). This completes the proof. ■

## APPENDIX C
## PROOF OF THEOREM 2

*Proof:* The expressions for $\lim_{N\to\infty} R^{\mathrm{ANOMA}}$ and $R^{\mathrm{NOMA}}$ are given by

$$\begin{aligned}
\lim_{N\to\infty} R^{\mathrm{ANOMA}} &= \log\left(\mu_1\mu_2 r_1\right) \\
&= \log\left\{\frac{1+\mu_1+\mu_2+\mu_1\mu_2(2\tau-2\tau^2)}{2}\right. \\
&\quad \left. + \frac{\sqrt{\left(1+\mu_1+\mu_2\right)^2 + 2\left(1+\mu_1+\mu_2\right)\mu_1\mu_2(2\tau-2\tau^2)}}{2}\right\}
\end{aligned} \tag{52}$$

and $R^{\mathrm{NOMA}} = \log(1+\mu_1+\mu_2)$, respectively.

If $\tau = 0$, it is easy to find that $\lim_{N\to\infty} R^{\mathrm{ANOMA}} = \log(1+\mu_1+\mu_2) = R^{\mathrm{NOMA}}$.

If $\tau \neq 0$, i.e., $\tau \in (0,1)$, we have $2\tau - 2\tau^2 > 0$. According to (52), since $\mu_1 > 0$ and $\mu_2 > 0$, we obtain

$$\begin{aligned}\lim_{N\to\infty} R^{\mathrm{ANOMA}} &= \log\left\{\frac{1+\mu_1+\mu_2+\mu_1\mu_2(2\tau-2\tau^2)}{2}\right.\\ &\quad\left.+\frac{\sqrt{(1+\mu_1+\mu_2)^2+2(1+\mu_1+\mu_2)\mu_1\mu_2(2\tau-2\tau^2)}}{2}\right\}\\ &> \log\left\{\frac{1+\mu_1+\mu_2}{2}+\frac{\sqrt{(1+\mu_1+\mu_2)^2}}{2}\right\} = R^{\mathrm{NOMA}}. \end{aligned} \tag{53}$$

Until now, we have proved $\lim_{N\to\infty} R^{\mathrm{ANOMA}} = R^{\mathrm{NOMA}}$ if $\tau = 0$ and $\lim_{N\to\infty} R^{\mathrm{ANOMA}} > R^{\mathrm{NOMA}}$ if $\tau \neq 0$. Next, we need to prove $\tau = 0$ if $\lim_{N\to\infty} R^{\mathrm{ANOMA}} = R^{\mathrm{NOMA}}$.

If $\lim_{N\to\infty} R^{\mathrm{ANOMA}} = R^{\mathrm{NOMA}}$, we have $\lim_{N\to\infty} R^{\mathrm{ANOMA}} = \log(\mu_1\mu_2 r_1) = \log(1+\mu_1+\mu_2) = R^{\mathrm{NOMA}}$.

After simplifications, we have

$$\sqrt{(1+\mu_1+\mu_2)^2+2(1+\mu_1+\mu_2)\mu_1\mu_2(2\tau-2\tau^2)} = 1+\mu_1+\mu_2-\mu_1\mu_2(2\tau-2\tau^2). \tag{54}$$

Note that (54) holds only if the right side of (54) is non-negative, i.e.,

$$1+\mu_1+\mu_2-\mu_1\mu_2(2\tau-2\tau^2) \geq 0. \tag{55}$$

Squaring both sides of the equal sign in (54), we obtain

$$4(1+\mu_1+\mu_2)(2\tau-2\tau^2) = \mu_1\mu_2(2\tau-2\tau^2)^2. \tag{56}$$

Then, (56) holds if $2\tau - 2\tau^2 = 0$ or $4(1+\mu_1+\mu_2) = \mu_1\mu_2(2\tau-2\tau^2)$. It is easy to prove that $4(1+\mu_1+\mu_2) = \mu_1\mu_2(2\tau-2\tau^2)$ contradicts (55). As a result, (56) holds only if $2\tau - 2\tau^2 = 0$ which then leads to $\tau = 0$.

Therefore, $\lim_{N\to\infty} R^{\mathrm{ANOMA}} \geq R^{\mathrm{NOMA}}$ is always true and the equal sign is achieved if and only if $\tau = 0$. This completes the proof. ■

## APPENDIX D
## PROOF OF THEOREM 3

*Proof:* From Theorem 1, we have

$$\begin{aligned} R^{\mathrm{ANOMA}} &= \frac{N}{N+\tau}\log\left(\mu_1\mu_2\right) + \frac{1}{N+\tau}\log\frac{(r_1^{N+1}-r_2^{N+1})+\tau^2(r_1^N-r_2^N)}{r_1-r_2} \\ &\overset{(a)}{=} \frac{N}{N+\tau}\log\left(\mu_1\mu_2\right) + \frac{1}{N+\tau}\log\left[\sum_{i=0}^{N} r_1^i r_2^{N-i} + \tau^2\sum_{i=0}^{N-1} r_1^i r_2^{N-1-i}\right] \\ &= \frac{1}{N+\tau}\log\left[\sum_{i=0}^{N} \mu_1^N\mu_2^N r_1^i r_2^{N-i} + \tau^2\sum_{i=0}^{N-1} \mu_1^N\mu_2^N r_1^i r_2^{N-1-i}\right] \\ &= \frac{1}{N+\tau}\log\left[\sum_{i=0}^{N} (\mu_1\mu_2)^{N-i}(\mu_1\mu_2 r_1)^i r_2^{N-i} + \tau^2\sum_{i=0}^{N-1} (\mu_1\mu_2)^{N-i}(\mu_1\mu_2 r_1)^i r_2^{N-1-i}\right], \end{aligned} \tag{57}$$

where $(a)$ is derived by applying $a^N - b^N = (a-b)(\sum_{i=0}^{N-1} a^i b^{N-1-i})$. In what follows, we prove that $r_2$ is a non-decreasing function of $\mu_1$ and $\mu_2$, and $\mu_1\mu_2 r_1$ increases as $\mu_1$ and $\mu_2$ increase, so that $R^{\mathrm{ANOMA}}$ increases as $\mu_1$ and $\mu_2$ increase.

From (17), we can find that $\frac{\partial r_1}{\partial \mu_1} < 0$ and $\frac{\partial r_1}{\partial \mu_2} < 0$. Since $r_2 = \tau^2(1-\tau)^2/r_1$, we further find that

$$\frac{\partial r_2}{\partial \mu_1} = -\frac{\tau^2(1-\tau)^2}{r_1^2}\frac{\partial r_1}{\partial \mu_1} \geqslant 0 \text{ and } \frac{\partial r_2}{\partial \mu_2} = -\frac{\tau^2(1-\tau)^2}{r_1^2}\frac{\partial r_1}{\partial \mu_2} \geqslant 0. \tag{58}$$

With (17), we have

$$\begin{aligned} \mu_1\mu_2 r_1 = &\frac{1+\mu_1+\mu_2+\mu_1\mu_2(2\tau-2\tau^2)}{2} \\ &+ \frac{\sqrt{\left(1+\mu_1+\mu_2\right)^2 + 2\left(1+\mu_1+\mu_2\right)\mu_1\mu_2(2\tau-2\tau^2)}}{2}. \end{aligned} \tag{59}$$

From (59), we can derive that

$$\frac{\partial(\mu_1\mu_2 r_1)}{\partial \mu_1} > 0 \text{ and } \frac{\partial(\mu_1\mu_2 r_1)}{\partial \mu_2} > 0. \tag{60}$$

Based on (58) and (60), we note that $r_2$ is a non-decreasing function of $\mu_1$ and $\mu_2$, and $\mu_1\mu_2 r_1$ increases as $\mu_1$ and $\mu_2$ increase. In addition, since $\mu_1$, $\mu_2$, $r_2$, and $\mu_1\mu_2 r_1$ are positive, the term $(\mu_1\mu_2)^j(\mu_1\mu_2 r_1)^i r_2^{M-i}$ ($i = 0, \cdots, M-1$, $j \geq 0$) is an increasing function of $\mu_1$ and $\mu_2$ for any positive $M$. Then, $R^{\mathrm{ANOMA}}$ is an increasing function of $\mu_1$ and $\mu_2$ because it is constituted by a sum of $(\mu_1\mu_2)^j(\mu_1\mu_2 r_1)^i r_2^{M-i}$ ($i = 0, \cdots, M-1$, $j \geq 0$, $M > 0$). Hence, maximizing the throughput is equivalent to maximizing $\mu_1$ and $\mu_2$ simultaneously, which means that the two users should transmit at full power. This completes the proof. ■

## APPENDIX E
## PROOF OF THEOREM 4

*Proof:*

$$\begin{aligned}\tau^* &= \arg\max_{\tau} \lim_{N\to\infty} R^{\mathrm{ANOMA}} = \arg\max_{\tau} \log\left(\mu_1\mu_2 r_1\right) \\ &= \arg\max_{\tau} \log\left\{\frac{1+\mu_1+\mu_2+\mu_1\mu_2(2\tau-2\tau^2)}{2}\right. \\ &\left. + \frac{\sqrt{\left(1+\mu_1+\mu_2\right)^2 + 2\left(1+\mu_1+\mu_2\right)\mu_1\mu_2(2\tau-2\tau^2)}}{2}\right\} \\ &\overset{(a)}{=} \arg\max_{\tau} \left[2\tau-2\tau^2\right] = 0.5, \end{aligned} \tag{61}$$

where $(a)$ is derived due to the fact that $\mu_1$ and $\mu_2$ are positive and independent of $\tau$. This completes the proof. ■

## REFERENCES


[1] X. Zou, B. He, and H. Jafarkhani, "On uplink asynchronous non-orthogonal multiple access systems with timing error," in *Proc. IEEE ICC*, Kansas City, MO, USA, May 2018, pp. 1–6.

[2] Z. Ding, X. Lei, G. K. Karagiannidis, R. Schober, J. Yuan, and V. K. Bhargava, "A survey on non-orthogonal multiple access for 5G networks: Research challenges and future trends," *IEEE J. Sel. Areas Commun.*, vol. 35, no. 10, pp. 2181–2195, Oct. 2017.

[3] X. Liu and H. Jafarkhani, "Downlink non-orthogonal multiple access with limited feedback," *IEEE Trans. Wireless Commun.*, vol. 16, pp. 6151–6164, Sep. 2017.

[4] D. Tse and P. Viswanath, *Fundamentals of wireless communication*. Cambridge university press, 2005.

[5] H. Jafarkhani, *Space-time coding: theory and practice*. Cambridge university press, 2005.

[6] S. Verdu, "The capacity region of the symbol-asynchronous Gaussian multiple-access channel," *IEEE Trans. Inf. Theory*, vol. 35, no. 4, pp. 733–751, Jul. 1989.

[7] X. Zou and H. Jafarkhani, "Asynchronous channel training in massive MIMO systems," in *Proc. IEEE GLOBECOM*, Washington, DC, USA, Dec. 2016, pp. 1–6.

[8] M. Ganji and H. Jafarkhani, "Interference mitigation using asynchronous transmission and sampling diversity," in *Proc. IEEE GLOBECOM*, Washington, DC, USA, Dec. 2016, pp. 1–6.

[9] H. Haci, H. Zhu, and J. Wang, "Performance of non-orthogonal multiple access with a novel asynchronous interference cancellation technique," *IEEE Trans. Commun.*, vol. 65, no. 3, pp. 1319–1335, Mar. 2017.

[10] A. Das and B. D. Rao, "MIMO systems with intentional timing offset," *EURASIP J. Adv. Signal Process.*, vol. 2011, no. 1, pp. 1–14, Dec. 2011.

[11] X. Zhang, M. Ganji, and H. Jafarkhani, "Exploiting asynchronous signaling for multiuser cooperative networks with analog network coding," in *Proc. IEEE WCNC*, San Francisco, CA, USA, Mar. 2017, pp. 1–6.

[12] X. Zhang and H. Jafarkhani, "Asynchronous network coding for multiuser cooperative communications," *IEEE Trans. Wireless Commun.*, vol. 16, no. 12, pp. 8250–8260, Dec. 2017.

[13] S. Poorkasmaei and H. Jafarkhani, "Asynchronous orthogonal differential decoding for multiple access channels," *IEEE Trans. Wireless Commun.*, vol. 14, no. 1, pp. 481–493, Jan. 2015.

[14] M. Avendi and H. Jafarkhani, "Differential distributed space-time coding with imperfect synchronization in frequency-selective channels," *IEEE Trans. Wireless Commun.*, vol. 14, no. 4, pp. 1811–1822, Apr. 2015.

[15] L. Lu and S. C. Liew, "Asynchronous physical-layer network coding," *IEEE Trans. Wireless Commun.*, vol. 11, no. 2, pp. 819–831, Feb. 2012.

[16] A. C. Marcum, J. V. Krogmeier, D. J. Love, and A. Sprintson, "Analysis and implementation of asynchronous physical layer network coding," *IEEE Trans. Wireless Commun.*, vol. 14, no. 12, pp. 6595–6607, Dec. 2015.

[17] Y. Shao, S. C. Liew, and L. Lu, "Asynchronous physical-layer network coding: Symbol misalignment estimation and its effect on decoding," *IEEE Trans. Wireless Commun.*, vol. 16, no. 10, pp. 6881–6894, Oct. 2017.

[18] J. Cui, G. Dong, S. Zhang, H. Li, and G. Feng, "Asynchronous NOMA for downlink transmissions," *IEEE Commun. Lett.*, vol. 21, no. 2, pp. 402–405, Oct. 2017.

[19] S. Parkvall, E. Strom, and B. Ottersten, "The impact of timing errors on the performance of linear DS-CDMA receivers," *IEEE J. Sel. Areas Commun.*, vol. 14, no. 8, pp. 1660–1668, Oct. 1996.

[20] H. Steendam and M. Moeneclaey, "The effect of synchronisation errors on MC-CDMA performance," in *Proc. of IEEE ICC*, Vancouver, BC, Canada, Jun. 1999, pp. 1510–1514.

[21] R. C. Palat, A. Annamalai, and J. H. Reed, "Accurate bit-error-rate analysis of bandlimited cooperative OSTBC networks under timing synchronization errors," *IEEE Trans. Veh. Technol.*, vol. 58, no. 5, pp. 2191–2200, Jun. 2009.

[22] S. Sesia, M. Baker, and I. Toufik, *LTE-the UMTS long term evolution: from theory to practice*. John Wiley & Sons, 2011.

[23] A. Goldsmith, S. A. Jafar, N. Jindal, and S. Vishwanath, "Capacity limits of MIMO channels," [Online], Available: https://web.stanford.edu/class/archive/ee/ee359/ee359.1062/cup_mimo.pdf.

[24] *Release 10: Physical Layer Procedures for Evolved Universal Terrestrial Radio Access (E-UTRA)*. document TS 36.213, v10.1.0, Apr. 2011.

[25] J. R. Magnus and H. Neudecker, *Matrix differential calculus with applications in statistics and econometrics*. NYC, NY: Wiley series in probability and mathematical statistics, 1988.

[26] J. D. Gibson, *Mobile communications handbook*. CRC press, 2012.

[27] D. Poole, *Linear algebra: A modern introduction*. Cengage Learning, 2014.